

Supporting Information

Tracking Areal Lithium Densities from Neutron Activation – Quantitative Li Determination in self-organized TiO₂ Nanotube Anode Materials for Li-ion Batteries

Engelbert Portenkirchner*, Giulia Neri, Josef Lichtinger, Jassen Brumbarov, Celine Rüdiger, Roman Gernhäuser, and Julia Kunze-Liebhäuser*

* Corresponding author: Tel.: +43-512-507-58014 Fax: +43-512-507-58199. E-mail address: Engelbert.Portenkirchner@uibk.ac.at (Engelbert Portenkirchner, DI (FH) Dr. techn.) and Tel.: +43-512-507-58013 Fax: +43-512-507-58199. E-mail address: Julia.Kunze@uibk.ac.at (Julia Kunze-Liebhäuser, Univ.-Prof. Dr.).

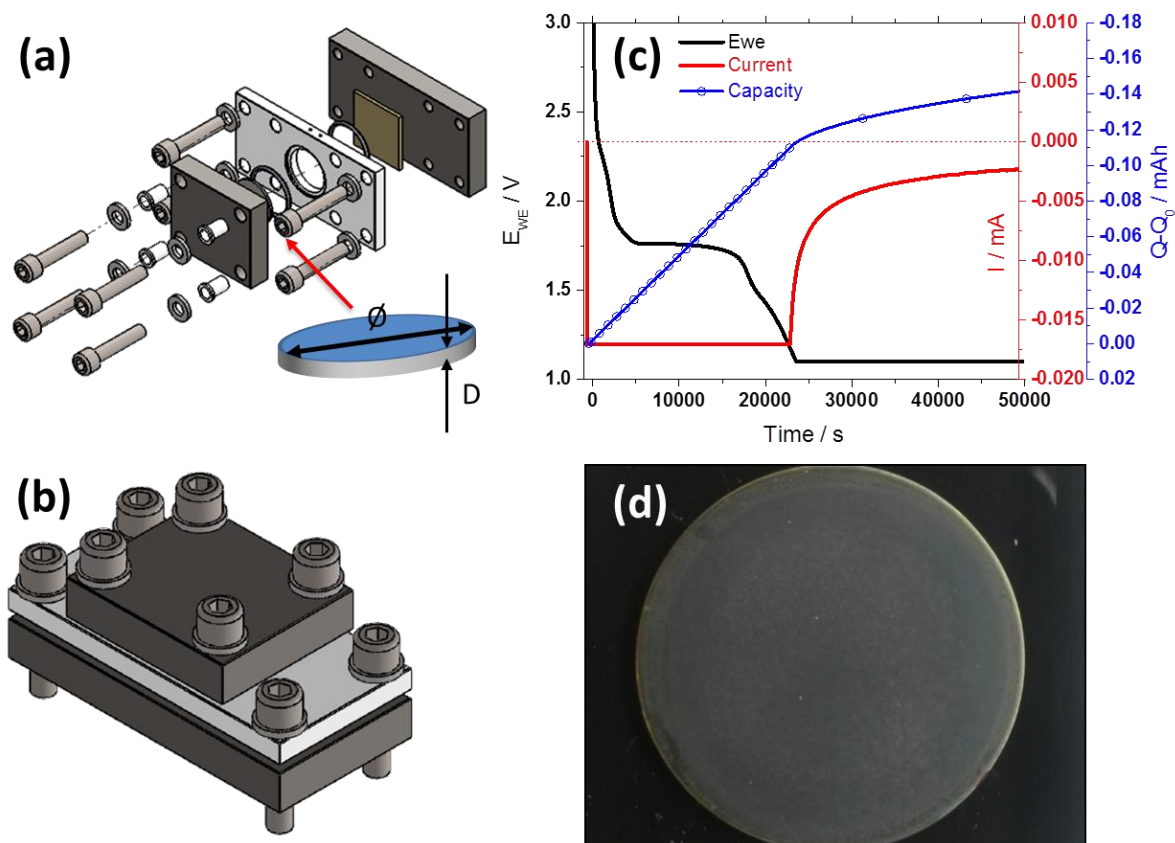


Figure S1. Electrochemical cell for lithiation: (a) Exploded view of the lithiation cell and position of the working electrode therein (not to scale), (b) isometric cell representation, (c) full lithiation: galvanostatically to 1.1 V, potentiostatically at 1.1 V to a steady-state current, (d) photograph of the working electrode: TiO_{2-x}-C NT on Ti-substrate, diameter (\varnothing) 20.00 (± 0.01 mm), thickness (D) 0.95 (± 0.02 mm).

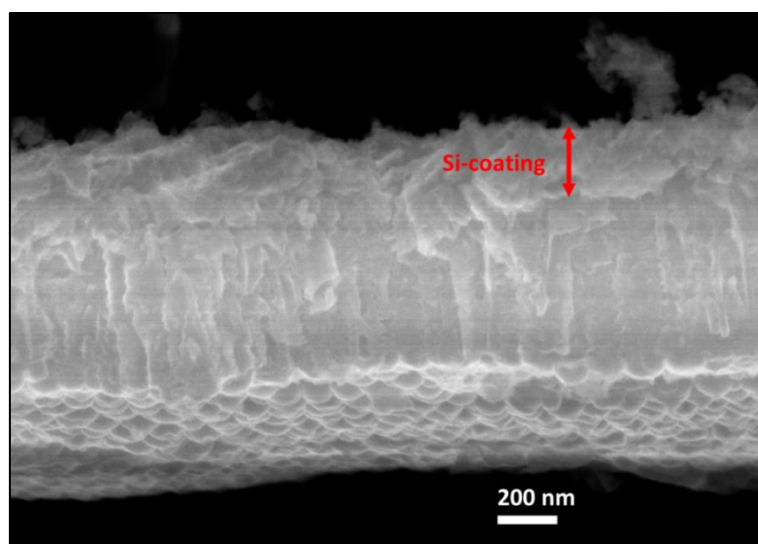


Figure S2. SE micrograph cross section of Si coated SiTiO_{2-x}-C NT after lithiation to 1.1 V.

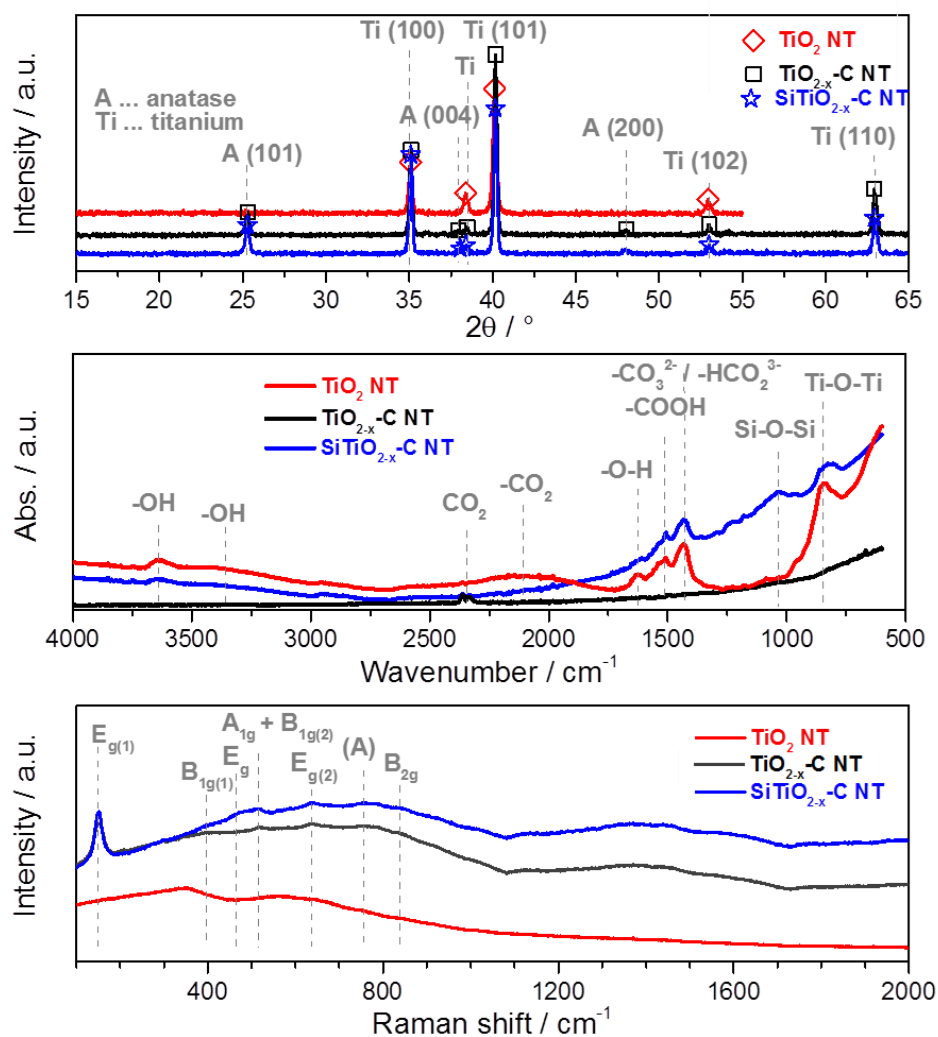


Figure S3. (a) XRD spectra, (b) ATR-FTIR spectra, and (c) Micro-Raman spectra of TiO₂ NT (red), TiO_{2-x}-C NT (black) and SiTiO_{2-x}-C NT (blue) before lithiation.

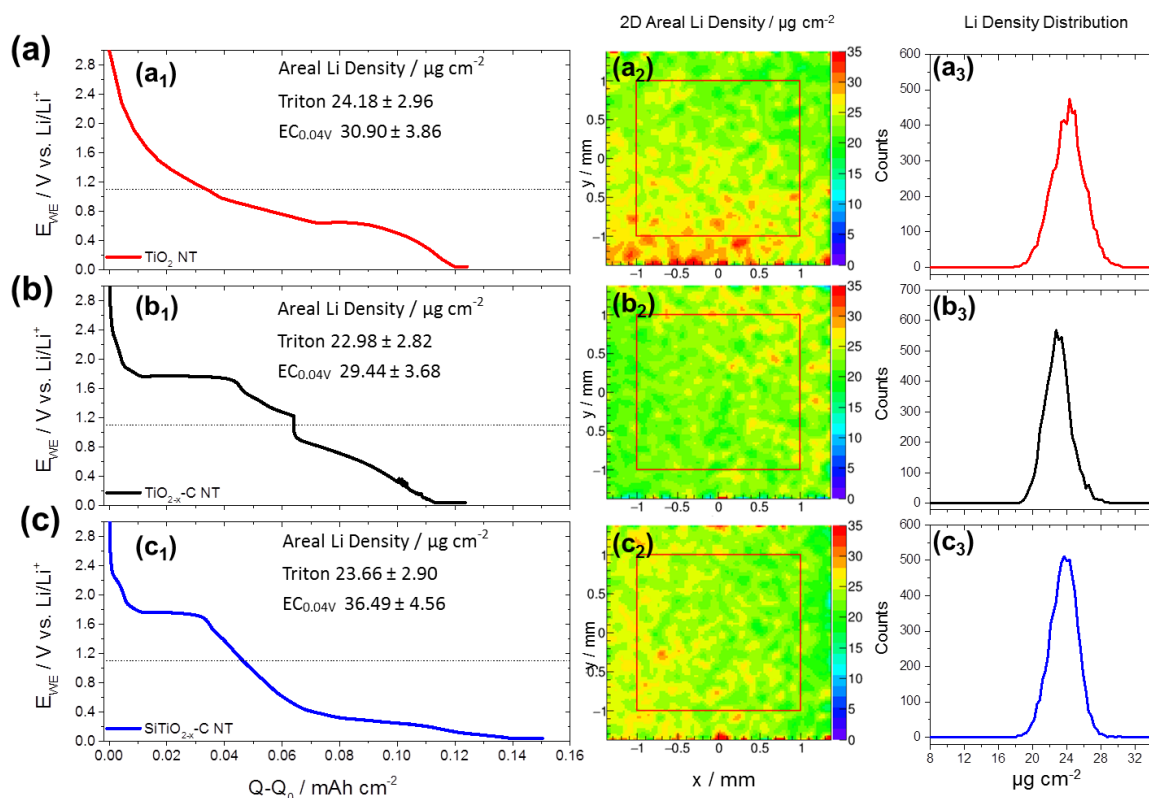


Figure S4. Galvanostatic lithiation to 0.04V (C/10), followed by potentiostatic lithiation at 0.04 V of (a₁) as grown TiO_2 NT, (b₁) anatase TiO_{2-x} -C NT, and (c₁) Si coated $SiTiO_{2-x}$ -C NT, (a₂-c₂) corresponding reconstructed areal Li density in $\mu g \text{ cm}^{-2}$ reduced to $2 \times 2 \text{ mm}^2$, (a₃-c₃) areal Li density distribution over the analyzed area.

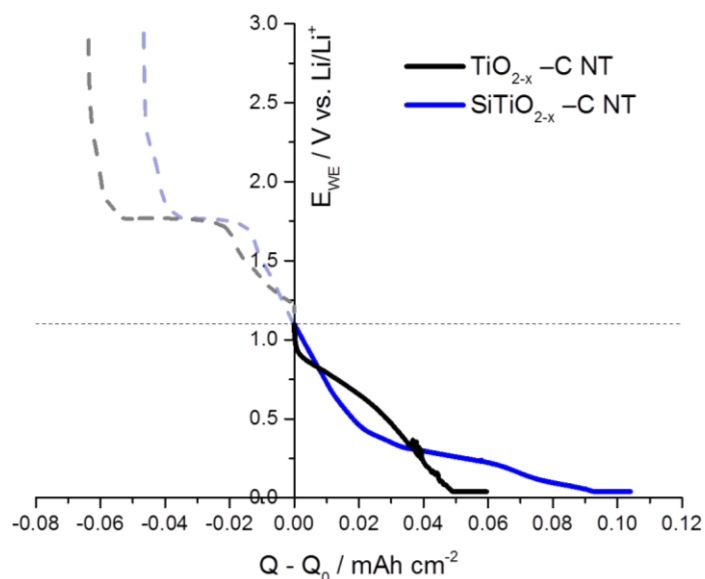


Figure S5. Comparison of TiO_{2-x} -C NT and $SiTiO_{2-x}$ -C NT lithiated to 0.04 V galvanostatically (C/10) and potentiostatically at 0.04 V. In this representation the 0 point for $Q - Q_0$ has intentionally been set to the point where the voltage drops below 1.1 V to highlight the post TiO_2 lithiation characteristics.

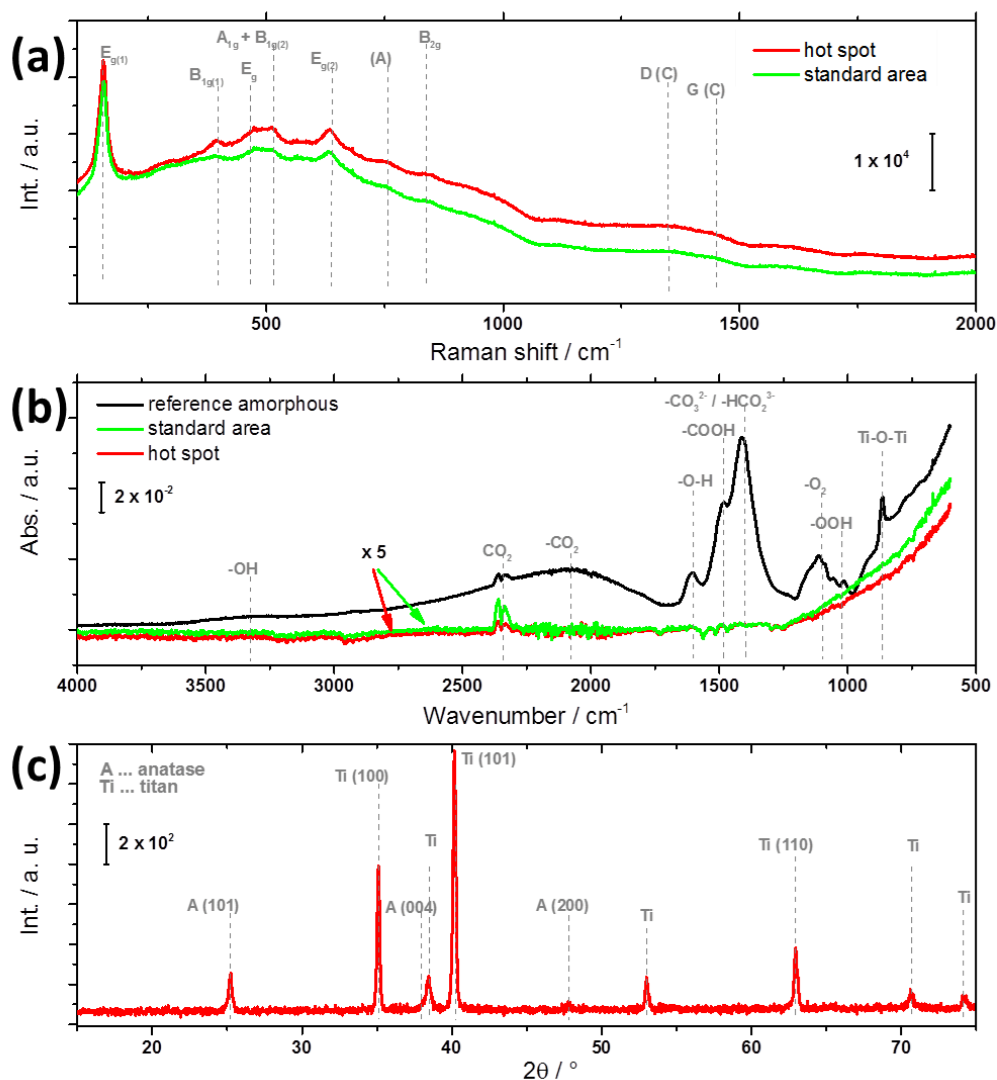


Figure S6. Spectroscopic analysis: (a) Micro-Raman spectra of areas with high Li concentration ('hot spot', red), and areas with standard Li concentration (green) after lithiation to 1.1 V. (b) ATR-FTIR spectra of areas with high Li concentration (red), and medium Li concentration (green) after lithiation. A reference measurement of an amorphous, as grown TiO_2 NT electrode after lithiation to 1.1 V is shown (black). For better comparability, the signals of the spectra with high and medium Li concentration have been increased by a factor of 5. (c) XRD spectra of $\text{SiTiO}_{2-x}\text{-C}$ NT after lithiation, showing anatase TiO_2 structure.

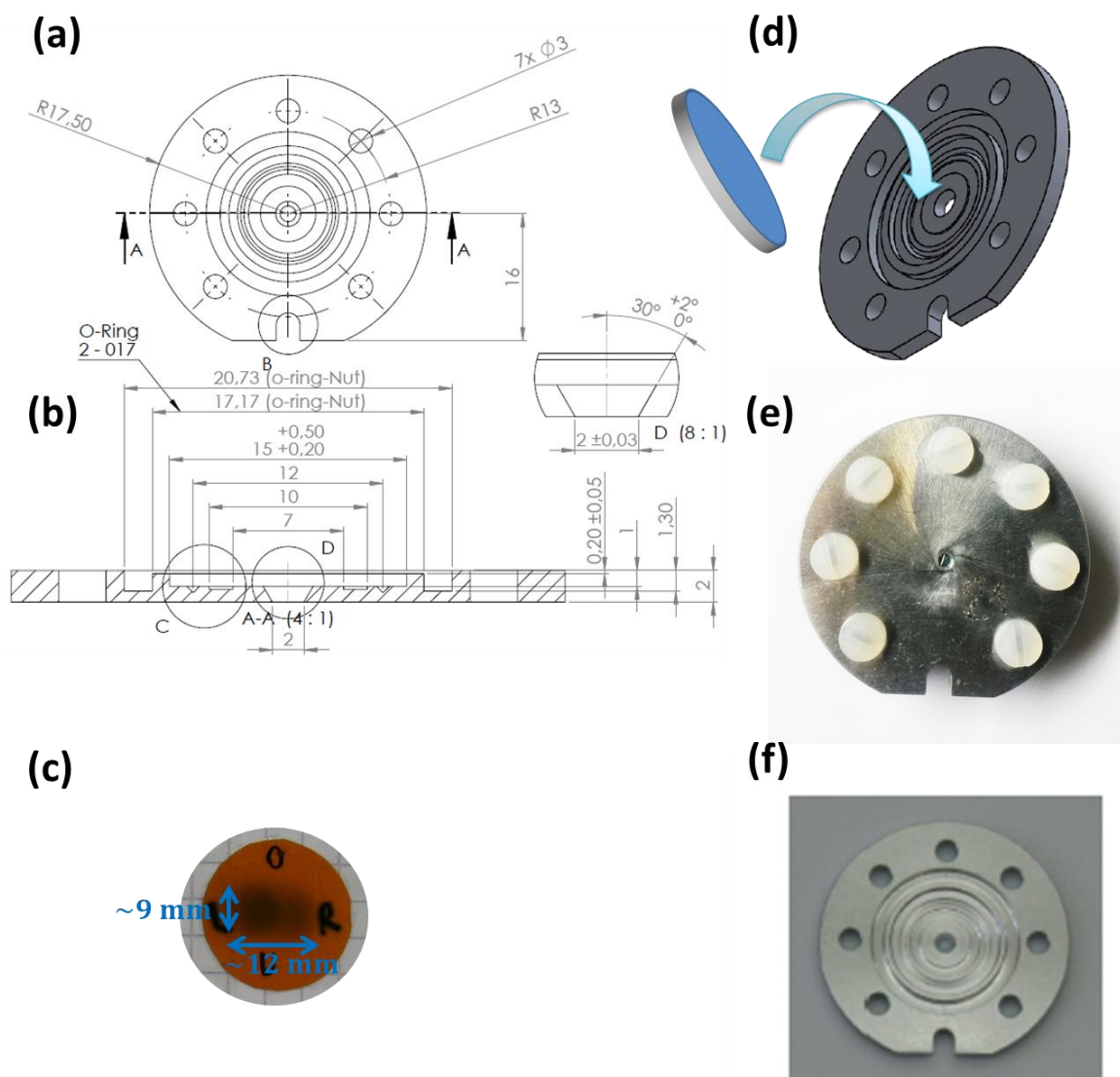


Figure S7. Target box for triton analysis with a pinhole aperture of 2 mm in the center (closed geometry), covered with an aluminium coated mylar foil. (a) technical drawing top view and (b) technical drawing for the cut through A to A in (a). (c) Cold neutron beam spot at the target position with an average neutron energy of 1.8 meV (6.7 \AA), a neutron flux of $2.7 \times 10^8 - 1.7 \times 10^{10} \text{ n cm}^{-2} \text{ s}^{-1}$ and a beam size of $9 \times 12 \text{ mm}$. (d) Isometric view of the target box and illustration of the positioning of the target sample therein. (e) real image of the fully assembled target box and (f), front aluminium plate with pinhole aperture in the mini-containers used for the TiO_2 NT samples.

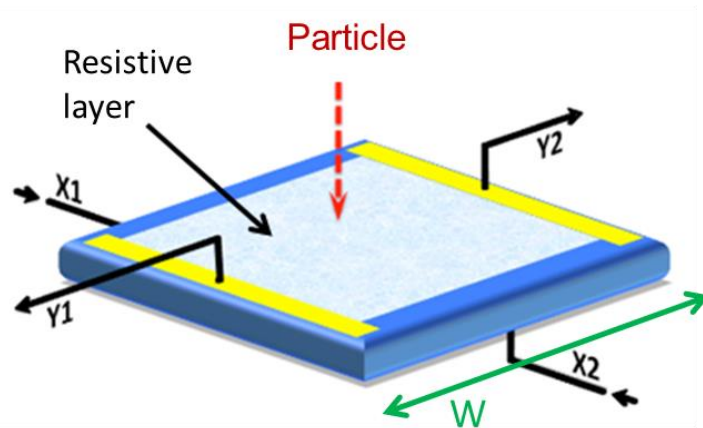


Figure S8. Position sensitive silicon detector with an intrinsic spatial detector resolution σ_{det} of $\sim 300 \mu\text{m}$ at 2 MeV. Final resolution depends on pinhole diameter and optical factor b/g . The impact position of particles on detector is given by: $x_{\text{det}} = \frac{W}{2} \cdot \frac{E_{x_1} - E_{x_2}}{E_{x_1} + E_{x_2}}$ and $y_{\text{det}} = \frac{W}{2} \cdot \frac{E_{y_1} - E_{y_2}}{E_{y_1} + E_{y_2}}$, where W is the detector width. The deposited energy is given by: $E_{y_1} + E_{y_2} = E_{x_1} + E_{x_2} = E$ and the emission position of particles in the target is given by: $x_{\text{target}} = -x_{\text{det}} \cdot \frac{g}{b}$, $y_{\text{target}} = -y_{\text{det}} \cdot \frac{g}{b}$, compare also Figure 7.

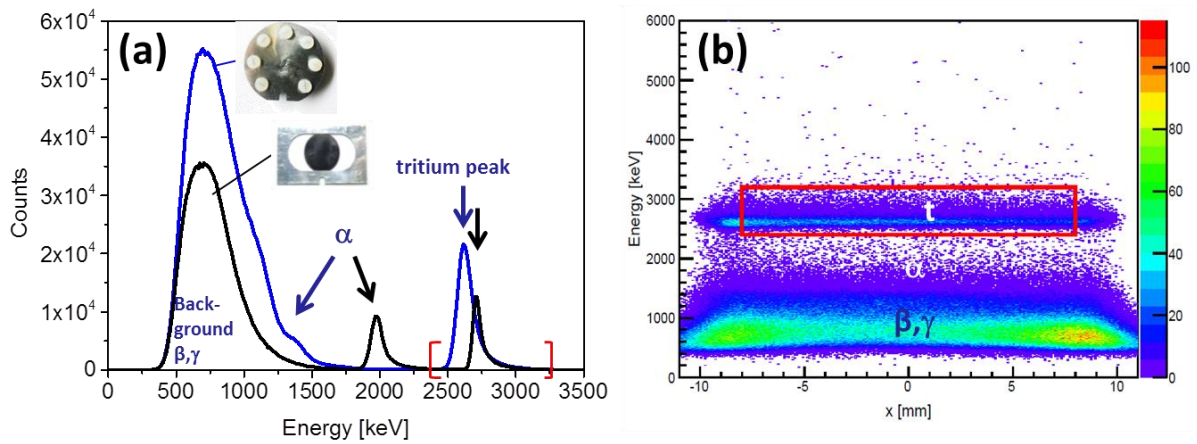


Figure S9. Calibration spectra of Li reference sample $\lambda_{\text{ref}} = 50 \mu\text{g LiF}_{\text{nat}} \text{ cm}^{-2}$ deposited on a Titanium blank for quantitative analysis. (a) Counts versus calibrated energy of the reference for the closed (blue) and open (black) sample holder. (b) Calibrated energy of particles hitting the detector vs. their impact position in x direction. Only tritium counts inside the red cut were used in the data analysis.